Underwater glider navigation error compensation using sea current data [★]

Jongrae Kim [*] **Yosup Park** [**] **Shinje Lee** [**] **Yong Kuk Lee** [**]

[*] *Biomedical Engineering/Aerospace Sciences, University Avenue, University of Glasgow, Glasgow G12 8QQ, UK (e-mail: Jongrae.Kim@glasgow.ac.uk).*
[**] *Korea Institute of Ocean Science & Technology, 787 Haean-ro, Sangnok-gu, Ansan-si, Gyeonggi-do, Republic of Korea (e-mail: yosup, sinje, yklee@kiost.ac)*

Abstract: Underwater glider is an emerging platform to explore the ocean with remarkably long operational endurance up to several months. Underwater glider navigation systems have significant limitations, on the other hand, in keeping the navigation error small. There is no reference coordinates information for position estimation and not enough immediate orientation reference for attitude estimation under the sea. Moreover, external disturbances including the sea currents make the navigation error increase further. In order to reduce the navigation error, we exploit a priori knowledge on the average current over the operation area. The performance and the robustness of the proposed algorithm are demonstrated using an experimental data obtained by Korea Institute of Ocean Science & Technology. The algorithm can be used to reduce the navigation error for one glider and also for multiple gliders by fusing the estimated errors. It can be also directly used to predict floating object path in order to use the prediction to design a collision avoidance path.

Keywords: Underwater Glider, Navigation Error, Floating Object, Collision Avoidance

1. INTRODUCTION

There has been a growing awareness of the ocean's roles in our life over the past few decades. In expanding our capabilities to acquire the knowledge of the world's oceans, the traditional observation platforms, for example, ships and mooring systems, have shown some limitations, which stem from high operation cost and some safety issues (Eriksen et al., 2001). On the other hand, UUV (Unmanned Underwater Vehicle) has proven to be an efficient tool for offshore resources exploration, maritime management, and naval defence with a lot less operation cost and almost free from any safety issues.

Two typical types of UUV are the one using screw propellers and the one using environmental energy, e.g., wave, wind, buoyancy gravity. UUV with propellers has accurate navigation capability and horizontal manoeuvrability but its operation time and the range are rather short, a few hours and less than 100km. UUV without propeller is called autonomous underwater glider. It has the global navigation and the vertical profiling manoeuvring capabilities with the monthly operation time and the long range over 1000km. Underwater gliders have clear advantages over the profiling floats because of active position control. Underwater gliders perform saw-tooth

trajectories from the surface to depths of 1000-1500m, along re-programmable routes using two-way communication via satellite. They can reach the forward speeds up to 40km/day, thanks to wings and rudders, and can be operated for a few months before they have to be recovered (Davis et al., 2002; Griffiths et al., 2001).

Gliders can record physical quantity, e.g., temperature and salinity, and biogeochemical quantity, such as pH, oxygen, and nitrate. At each surfacing, the collected data is sent to the land operation centre and new commands are received, if necessary, via the bidirectional Iridium satellite communication system at the rate of 30 to 60Kbytes for 5 minutes in every 4 to 5 hours. Underwater glider has so many advantages including long term mission, controlled navigation, profiling capabilities, easy deploy & recovery operation, and satellite communication. They could be used to monitor key regions in the world, where one needs to collect data with a higher resolution than presently available (Testor et al., 2009).

Despite of these advantages of underwater glider, its navigation system inherently includes large propagation errors, which present for almost all underwater vehicles. Just in a few meters below the surface of water, no reference signals, e.g. GPS (Global Positioning System), are available for correcting navigation system error. To reduce the navigation errors in the dead-reckoning navigation, the usage of regional current model was presented in (Smith et al., 2010). We further develop this idea by establishing the navigation error models and implementing algorithms to compensate the errors. The accelerometer bias error is to
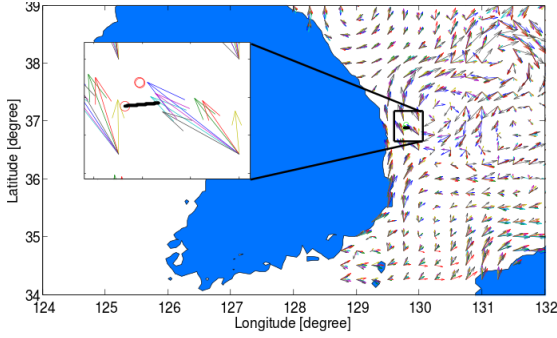
Fig. 1. The experiment was performed in East Sea indicated by the rectangular box. The arrows are the average current velocity at each location for seven different dates from 11th to 17th March of 2011 (Korea Hydrographic & Oceanographic Administration, 2011). The red circles in the inset box are the position information from GPS and the black thick line is the path obtained by the estimator designed in Section 3.

be completed and the position is obtained by correcting the acceleration measurement further using an average sea current velocity data.

KIOST (Korea Institute of Ocean Science & Technology) has been operating underwater gliders since 2011. The first flight was crossing East Sea during 6 days, where the eddy current of 1kt was present, and touching down 200m depth while sound velocity and temperature profiling at every 5 seconds (Imlach and Mahr, 2012; Park et al., 2012). All the experimental data presented in the following were obtained during this operation in the region shown in Figure 1 using Exocetus Coastal Glider, LG19 (Exocetus, 2013; Imlach and Mahr, 2012). Its diameter and length are 32.4cm and 2.87m, respectively, and its weight is 109kg. It is equipped with an IMU (Inertial Measurement Unit), which provides heading, roll and pitch angles, position, velocity, and acceleration of the glider.

In the following, Section 2, the navigation equation is derived and the navigation sensor output is characterised. In Section 3, the major navigation error sources are modelled and the error correction algorithms using the built-in navigation system output and the average sea current data are presented. The performance of the algorithms are demonstrated using a field data collected by KIOST. Finally, the conclusions are presented.

2. NAVIGATION SYSTEM

2.1 Relative Motion Equation

The relation among the position vector of the underwater glider, $\mathbf{r}_b$, the sensor position in the body-coordinates ($\mathcal{B}$), $\mathbf{r}_s$, and the one in the reference-coordinates ($\mathcal{R}$), $\mathbf{r}$, is shown in Figure 2 and given by

$$\mathbf{r} = \mathbf{r}_b + \mathbf{r}_s \qquad (1)$$

More explicitly with the coordinates expressed,

$$\mathbf{r}_b = \mathbf{r}^{\mathcal{B}} - \mathbf{r}_s^{\mathcal{B}} \qquad (2)$$

where $\mathbf{r}_b$ is the position vector expressed by two vectors in the right hand side, and $\mathcal{B}$ in the superscripts is indicated that both vectors are expressed in the body-coordinates.
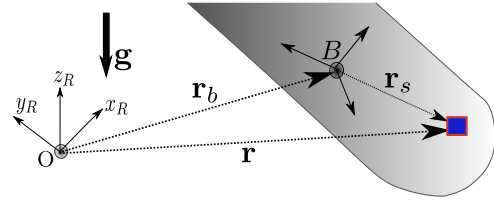

Fig. 2. The origins of the reference-coordinates and the body-coordinates are indicated by O and B, respectively. The body coordinates is attached to the glider and $\mathbf{r}_s$ is the sensor position vector relative to the origin of the body-coordinates. $\mathbf{g}$ is the gravitational acceleration vector.

Take the time-derivative of (2) and obtain the velocity,

$$\mathbf{v}_b = \frac{d}{dt}\mathbf{r}_b = \frac{d}{dt}\mathbf{r}^{\mathcal{B}} - \boldsymbol{\omega} \times \mathbf{r}_s^{\mathcal{B}} \qquad (3)$$

where $\dot{\mathbf{r}}_s^{\mathcal{B}}$ is zero because the glider is assumed to be a rigid-body, and the following transport theorem is used in the derivative (Schaub and Junkins, 2009).

Theorem 1. (Transport Theorem) The time derivative of a generic vector, $\mathbf{x}$, which is expressed in the rotating coordinates with the angular velocity, $\boldsymbol{\omega}$, with respect to the inertial coordinates is

$$\frac{d^{\mathcal{R}}}{dt}\mathbf{x}^{\mathcal{B}} = \frac{d^{\mathcal{B}}}{dt}\mathbf{x}^{\mathcal{B}} + \boldsymbol{\omega}^{\mathcal{B}} \times \mathbf{x}^{\mathcal{B}}$$

or simply

$$\frac{d^{\mathcal{R}}}{dt}\mathbf{x} = \dot{\mathbf{x}} + \boldsymbol{\omega} \times \mathbf{x} \qquad (4)$$

where $\times$ is the vector cross product.

Proof: The proof is omitted and it can be found in (Schaub and Junkins, 2009). ∎

Note that the first term in the right-hand side of (3) is not expanded using the Transport theorem. Later, it will be directly obtained from the accelerometer attached at $\mathbf{r}_s$ in the glider.

Take one more time-derivative of (3)

$$\mathbf{a}_b = \frac{d}{dt}\mathbf{v}_b = \frac{d^2}{dt^2}\mathbf{r} - \dot{\boldsymbol{\omega}} \times \mathbf{r}_s - \boldsymbol{\omega} \times (\boldsymbol{\omega} \times \mathbf{r}_s) \qquad (5)$$

where the superscript, $\mathcal{B}$, in the terms in the right hand side is dropped for brevity, and they are all expressed in the body-coordinates.

2.2 Navigation Equation

The following quantity, $\mathbf{a}_{\text{acc}}^{\mathcal{B}}$, can be measured by the 3-axis accelerometer in the glider:

$$\mathbf{a}_{\text{acc}}^{\mathcal{B}} = \ddot{\mathbf{r}} + C_{\mathcal{R}}^{\mathcal{B}}(\psi, \theta, \phi)\mathbf{g}^{\mathcal{R}} \qquad (6)$$

where $\mathbf{a}_{\text{acc}}^{\mathcal{B}}$ is the acceleration information expressed in the body-coordinates, $\ddot{\mathbf{r}}$ is equal to $d^2\mathbf{r}/dt^2$, $C_{\mathcal{R}}^{\mathcal{B}}(\psi, \theta, \phi)$ is the direction cosine matrix, which changes the coordinates from the reference to the body with the rotating sequence given by yaw(ψ), pitch(θ), and roll(ϕ), $\mathbf{g}^{\mathcal{R}} = [0, 0, -g]^T$, the gravitational acceleration expressed in the reference coordinates, and $g = 9.821$ m/s^2.

Substitute $d^2\mathbf{r}/dt^2$ in (5) by the expression in (6)

$$\mathbf{a}_b = \frac{d}{dt}\mathbf{v}_b = \mathbf{a}_{\text{acc}}^{\mathcal{B}} - C_{\mathcal{R}}^{\mathcal{B}}\mathbf{g}^{\mathcal{R}} - \dot{\boldsymbol{\omega}} \times \mathbf{r}_s - \boldsymbol{\omega} \times (\boldsymbol{\omega} \times \mathbf{r}_s) \quad (7)$$
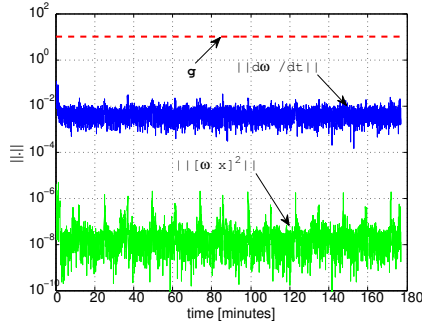
Fig. 3. The norms of angular acceleration and squared angular velocity cross product operator are about 100 times or 100 million times smaller than the gravitational acceleration.

In a matrix operation format, it can be written as

$$\mathbf{a}_b = \frac{d}{dt}\mathbf{v}_b = \mathbf{a}_{\text{acc}}^{\mathcal{B}} - C_{\mathcal{R}}^{\mathcal{B}}\mathbf{g}^{\mathcal{R}} - [\dot{\boldsymbol{\omega}}\times]\mathbf{r}_s - [\boldsymbol{\omega}\times]^2\mathbf{r}_s \quad (8)$$

where

$$[\boldsymbol{\omega}\times] := \begin{bmatrix} 0 & -\omega_3 & \omega_2 \\ \omega_3 & 0 & -\omega_1 \\ -\omega_2 & \omega_1 & 0 \end{bmatrix}, \quad (9)$$

ω_i for $i = 1, 2, 3$ is the angular velocity for each axis in the body-coordinates, and $[\dot{\boldsymbol{\omega}}\times]$ is defined in the similar manner.

Rotational angular velocity of underwater vehicle is, in general, very slow, i.e. $\|\boldsymbol{\omega}\|$ and $\|\dot{\boldsymbol{\omega}}\|$ are much smaller than $\|\mathbf{g}\|$. Figure 3 shows that in the experiment the magnitudes of two terms are at least 100-times smaller than the magnitude of the gravitational acceleration. Note that the angular acceleration is calculated by finite-difference using the angular rate measurement. In addition, $\|\mathbf{r}_s\|$ is less than 1m and $\|C_{\mathcal{R}}^{\mathcal{B}}\|$ is equal to 1. Hence, the angular velocity related terms in (8) can be ignored and the acceleration becomes

$$\mathbf{a}_b \approx \mathbf{a}_{\text{acc}}^{\mathcal{B}} - C_{\mathcal{R}}^{\mathcal{B}}\mathbf{g}^{\mathcal{R}} \quad (10)$$

After transforming the coordinates of (10) into the reference-coordinates, integrating it with respect to time provides the velocity expressed in the reference frame as follows:

$$\mathbf{v}_b^{\mathcal{R}}(t) = C_{\mathcal{B}}^{\mathcal{R}}(t_0)\mathbf{v}_b^{\mathcal{B}}(t_0) + \int_{t_0}^{t} C_{\mathcal{B}}^{\mathcal{R}}(\tau)\mathbf{a}_b^{\mathcal{B}}(\tau)d\tau \quad (11)$$

where t_0 is the initial time, $C_{\mathcal{B}}^{\mathcal{R}}(t_0)$ is the initial attitude, $\mathbf{v}_b^{\mathcal{B}}(t_0)$ is the initial velocity, and in order to emphasise the dependency to time each term in the above is written as a function of time. Note that $C_{\mathcal{B}}^{\mathcal{R}}$ is equal to the transpose of $C_{\mathcal{R}}^{\mathcal{B}}$.

Finally, the glider position in the reference frame is obtained by

$$\mathbf{r}_b^{\mathcal{R}}(t) = \mathbf{r}_b^{\mathcal{R}}(t_0) + \int_{t_0}^{t} \mathbf{v}_b^{\mathcal{R}}(\tau)d\tau \quad (12)$$

where $\mathbf{r}_b^{\mathcal{R}}(t_0)$ is the initial position of the glider.

2.3 Navigation Algorithm & Sensor Output

Exocetus Coastal glider has a built-in navigation algorithm and it records various navigation data. The following discussions are based on the log-file obtained from the glider navigation system. The 3-Axis Acceleration measurements expressed in the body-coordinates, $\tilde{\mathbf{a}}_{\text{acc}}^{\mathcal{B}}$, are directly available from the log-file and it can be expressed as follows:

$$\tilde{\mathbf{a}}_{\text{acc}} = \tilde{\ddot{\mathbf{r}}} + \mathbf{C}_{\mathcal{R}}^{\mathcal{B}}(\psi, \theta, \phi)\mathbf{g}^{\mathcal{R}} + \mathbf{b}_{\text{acc}} + \mathbf{n}_{\text{acc}} \quad (13)$$

where $\tilde{\ddot{\mathbf{r}}}$ is the measured quantity by the calibrated accelerometer if there is no stochastic noise and bias error, $\mathbf{b}_{\text{acc}}$ is the accelerometer sensor bias error, $\mathbf{n}_{\text{acc}}$ is the white noise, and the accelerations caused by the control forces and the external disturbances are all included in $\ddot{\mathbf{r}}$. Usually, in the estimation problem, $\tilde{\ddot{\mathbf{r}}}$ is assumed to equal to $\ddot{\mathbf{r}}$, which presumes infinite resolution and infinitesimal time constant, i.e. a perfect sensitivity. In reality, including the limitations in the resolution and the finite response time, and some unknown error sources, $\tilde{\ddot{\mathbf{r}}}$ will be different from $\ddot{\mathbf{r}}$ (Ulanov, 2006).

The navigation algorithm provides the attitude information, which includes some errors, $\delta\psi$, $\delta\theta$, and $\delta\phi$, then

$$C_{\mathcal{R}}^{\mathcal{B}} = C_{\mathcal{B}'}^{\mathcal{B}}(\delta\psi, \delta\theta, \delta\phi)\, C_{\mathcal{R}}^{\mathcal{B}'}(\tilde{\psi}, \tilde{\theta}, \tilde{\phi}) \quad (14)$$

where $\mathcal{B}'$ is the body-coordinates that the navigation system calculated, $\tilde{\psi}, \tilde{\theta}, \tilde{\phi}$ are roll, pitch and yaw angles returned from the navigation algorithm, and $\delta\psi, \delta\theta, \delta\phi$ are the attitude angles of the true body-coordinates, $\mathcal{B}$, with respect to the calculated body-coordinates, $\mathcal{B}'$. With the small angle assumption, i.e., $\delta\psi \ll 1$, $\delta\theta \ll 1$, and $\delta\phi \ll 1$,

$$C_{\mathcal{B}'}^{\mathcal{B}}(\delta\psi, \delta\theta, \delta\phi) \approx \begin{bmatrix} 1 & \delta\psi & \delta\theta \\ -\delta\psi & 1 & \delta\phi \\ \delta\theta & -\delta\phi & 1 \end{bmatrix} \quad (15)$$

In addition, the navigation system log-file provides the velocity and the position estimations in the reference coordinates, i.e., $\hat{\mathbf{v}}_b^{\mathcal{R}}(t)$ and $\hat{\mathbf{r}}_b^{\mathcal{R}}(t)$.

3. NAVIGATION ERROR REDUCTION

There are three major error sources in the acceleration estimation: physical sensor limitation in the accelerometer($\Delta\ddot{\mathbf{r}}$); orientation error (ΔC); and the accelerometer bias ($\mathbf{b}_{\text{acc}}$). The detail algorithm of the glider navigation system is unknown but in general the orientation error can be kept quite small. The glider has the magnetometer and it could provide reasonably good heading information. Moreover, whenever the angular velocity remains roughly constant during a certain time interval, then the direction of the gravitational vector can be estimated. Using these two vectors, the standard orientation estimation algorithm, e.g. QUEST (Quaternion Estimation) (Shuster and Oh, 1981), with Kalman Filter (Lefferts et al., 1982), would work very well in minimising the attitude estimation error.

Hence, the navigation system returns reasonably accurate orientation information, $C_{\mathcal{B}'}^{\mathcal{B}} \approx I_3$, where I_3 is the 3x3 identity matrix. For example, the Slocum glider attitude error is around $\pm 1°$ in heading accuracy and $\pm 0.2°$ in roll and pitch accuracy (Smith et al., 2010). In addition, the accelerometer sensor bias, $\mathbf{b}_{\text{acc}}$, would be well-estimated a priori and compensated during a sensor calibration procedure. Hence, the velocity and the position estimation from the built-in navigation system would be free from the accelerometer bias. However, the navigation log file does not provide the bias corrected accelerometer measurements
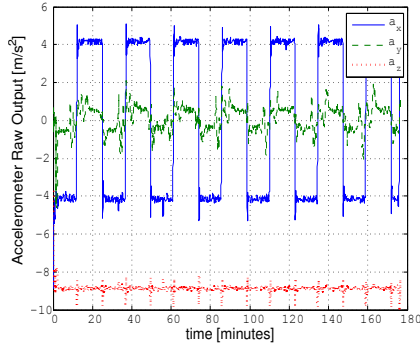
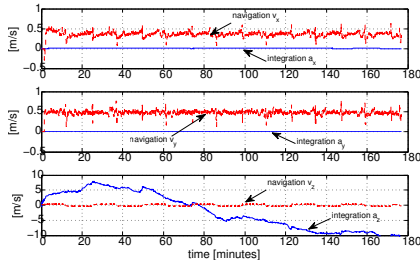Fig. 4. Raw accelerometer measurements output

Fig. 5. Comparison between the integration of the accelerometer measurements output and the velocity information from the navigation system
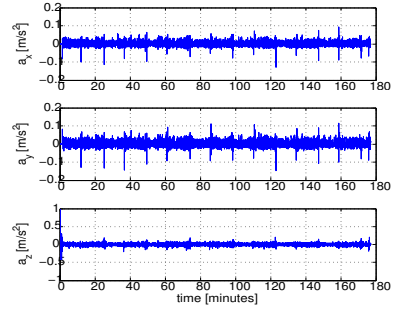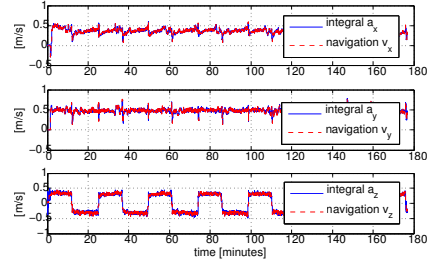

Fig. 6. Bias corrected acceleration measurement

Fig. 7. Comparison between the integration of the corrected acceleration and the velocity information from the navigation system

3.2 Error Correction Using Navigation Data

If the accelerometer output is directly integrated after the gravitational effect is removed using the attitude information, the velocity is still very different from the one from the navigation system as shown in Figure 5.

Using the accelerometer output, the velocity can be written as follows:

$$\dot{\mathbf{v}} = C_{\mathcal{B}}^{\mathcal{R}} \mathbf{a}_b = C_{\mathcal{B}'}^{\mathcal{R}} C_{\mathcal{B}}^{\mathcal{B}'} \left(\hat{\mathbf{a}}_b + \delta \mathbf{a}_b \right)$$
$$= C_{\mathcal{B}'}^{\mathcal{R}} \left(I + \Delta C \right) \left(\hat{\mathbf{a}}_b + \delta \mathbf{a}_b \right) \qquad (21)$$

and it can be further expanded

$$\dot{\mathbf{v}} = C_{\mathcal{B}'}^{\mathcal{R}} \left(\hat{\mathbf{a}}_b + \Delta C \hat{\mathbf{a}}_b + \delta \mathbf{a}_b + \Delta C \delta \mathbf{a}_b \right) \qquad (22)$$

Let

$$\mathbf{w} = -C_{\mathcal{B}'}^{\mathcal{R}} \left(\Delta C \hat{\mathbf{a}}_b + \delta \mathbf{a}_b + \Delta C \delta \mathbf{a}_b \right) \qquad (23)$$

then,

$$\dot{\mathbf{v}} = C_{\mathcal{B}'}^{\mathcal{R}} \hat{\mathbf{a}}_b - \mathbf{w} \qquad (24)$$

Assume $\mathbf{w}$ be approximated as a piecewise constant, i.e., the following is satisfied almost every instant:

$$\dot{\mathbf{w}} \approx \mathbf{0} \qquad (25)$$

Hence, the navigation equation for each axis is given by

$$\dot{\mathbf{x}} = A\mathbf{x} + Bu \qquad (26)$$

where u is the i-axis component of $C_{\mathcal{B}'}^{\mathcal{R}} \hat{\mathbf{a}}_b$,

$$\mathbf{x} = \begin{bmatrix} p_i & v_i & w_i \end{bmatrix}^T \qquad (27)$$

for $i = x, y$ or z, p_i is the i-axis coordinate of the glider in the reference frame, v_i is the i-axis velocity of the glider in the reference frame, w_i is the i-axis error in the accelerometer measurement projecting on the reference frame, and

$$A = \begin{bmatrix} 0 & 1 & 0 \\ 0 & 0 & -1 \\ 0 & 0 & 0 \end{bmatrix}, \ B = \begin{bmatrix} 0 \\ 1 \\ 0 \end{bmatrix} \qquad (28)$$

but the raw measurement including the gravitational acceleration. Therefore, $\mathbf{b}_{\text{acc}}$ and $\Delta \ddot{\mathbf{r}}$ are the unknowns to be estimated.

In the following, firstly, we estimate the bias in the acceleration measurement using the navigation system output and secondly, $\Delta \ddot{\mathbf{r}}$ will be reduced using the average sea current data. The performance of the algorithms will be verified using the GPS updated position information.

3.1 Accelerometer Error Model

The acceleration of the glider, (10), is calculated as follows:

$$\hat{\mathbf{a}}_b = \tilde{\mathbf{a}}_{\text{acc}}^{\mathcal{B}} - C_{\mathcal{R}}^{\mathcal{B}'} \mathbf{g}^{\mathcal{R}} \qquad (16)$$

where the raw measurement from the experiment, $\tilde{\mathbf{a}}_{\text{acc}}^{\mathcal{B}}$, is shown in Figure 4.

The error between (10) and (16) is defined by

$$\delta \mathbf{a}_b = \hat{\mathbf{a}}_b - \mathbf{a}_b = \Delta \ddot{\mathbf{r}} + \Delta C \, \mathbf{g}^{\mathcal{B}'} + \mathbf{b}_{\text{acc}} + \mathbf{n}_{\text{acc}} \qquad (17)$$

where

$$\Delta \ddot{\mathbf{r}} = \tilde{\ddot{\mathbf{r}}} - \ddot{\mathbf{r}} \qquad (18)$$

$$\Delta C = \begin{bmatrix} 0 & \delta\psi & \delta\theta \\ -\delta\psi & 0 & \delta\phi \\ \delta\theta & -\delta\phi & 0 \end{bmatrix}, \qquad (19)$$

$\mathbf{g}^{\mathcal{B}'}$ is the gravitational acceleration expressed in $\mathcal{B}'$, and $\delta\psi$, the yaw angle error does not affect to the projection of the gravitational vector on the body-coordinates ($\mathcal{B}'$). Hence,

$$\mathbf{g}^{\mathcal{B}'} = g \left[-\sin\tilde{\theta}, \ \sin\tilde{\phi}\cos\tilde{\theta}, \ \cos\tilde{\phi}\cos\tilde{\theta} \right]^T \qquad (20)$$

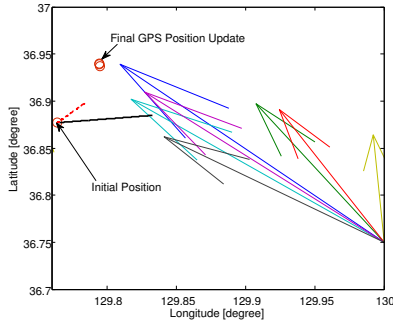where $(\cdot)^T$ is the transpose of the vector.

Fig. 8. Paths obtained by integrating the bias error only (black solid line), and the bias with the sea current drag fixed (red dashed line) accelerometer measurement. Initial and the final position update using GPS are indicated by the red circles and the coloured arrows are the average current for seven different dates.

Hence, the corresponding estimator is

$$\dot{\hat{\mathbf{x}}} = A\hat{\mathbf{x}} + B\mathbf{u} + K_{\text{obs}}\left(C\hat{\mathbf{x}} - \tilde{\mathbf{y}}\right) \qquad (29)$$

where K_{obs} is the observer gain to be designed,

$$C = \begin{bmatrix} 1 & 0 & 0 \\ 0 & 1 & 0 \end{bmatrix}, \quad \tilde{\mathbf{y}} = \begin{bmatrix} p_i^{\text{nav}} \\ v_i^{\text{nav}} \end{bmatrix} \qquad (30)$$

and p_i^{nav} and v_i^{nav} are the position and the velocity information of i-axis from the navigation system. In order to make the error dynamics of the estimator stable, i.e., the real parts of all eigenvalues of $A + K_{\text{obs}}C$ being negative, the following gain is chosen by trial and error:

$$K_{\text{obs}} = -5 \begin{bmatrix} 1 & 1 \\ 0 & 1 \\ 0 & -1 \end{bmatrix} \qquad (31)$$

Using $\mathbf{w}$ from the estimator, (29), the acceleration, $\dot{\mathbf{v}}$, is calculated from (24) and it is shown in Figure 6. In order to verify whether these acceleration would be close to the true, the acceleration is numerically integrated and it provides the velocity. The velocity is compared with the velocity information from the navigation system in Figure 7. As shown in the figure, two quantities are almost identical and we can conclude that the acceleration calculated is at least as much accurate as the acceleration information that the navigation system has.

3.3 Error Correction Using Average Sea Current

Once the bias correction is completed, the position information can be obtained by integrating the corrected accelerometer output twice. The integrated path is shown in Figure 8 indicated in the black solid line. The starting position was initialised by the GPS signal and it has an accurate starting position information. However, because of $\Delta\ddot{\mathbf{r}}$ error effects accumulated during the diving, the position at the end just before it is updated by GPS again has several km error after about 3 hours operation under the water, as shown in Figure 8. The main cause of this error might be the current as the final position is almost exactly drifted towards the directions where the average current flows. The similar drifts are observed in another three diving (Alaks Native Technologies, 2011).

The question is why the force caused by the current is not included in the accelerometer measurement. To quantify how much acceleration would be generated from
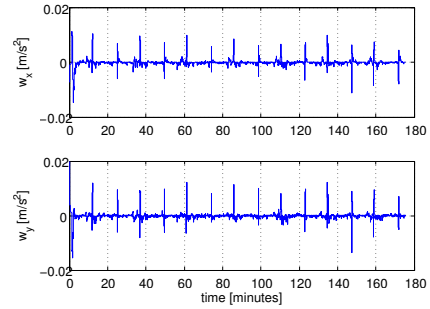

Fig. 9. Acceleration in the East and the North directions caused by the current drag force

the current, the following equation is used (Sherman et al., 2001):

$$D = \frac{1}{2}\rho \, \|\Delta\mathbf{v}\|^2 \, A_D C_D \qquad (32)$$

where ρ is the sea water density, which is around 1020 kg/m^3, $\Delta\mathbf{v}$ is the relative velocity of the glider in the horizontal plane, i.e.

$$\Delta\mathbf{v} = \begin{bmatrix} v_E^{\text{crt}} & v_N^{\text{crt}} & 0 \end{bmatrix}^T - \begin{bmatrix} v_x & v_y & 0 \end{bmatrix}^T, \qquad (33)$$

v_E^{crt} and v_N^{crt} are the sea current velocity in the east or the north direction, respectively, whose magnitude is around 1kt ($\approx$ 0.5 m/s) in the maximum, A_D is the cross section area of the glider hull, which is about 824 cm^2, and C_D is the drag coefficient set to 0.4, which is adopted from (Sherman et al., 2001). Unlike the example shown in (Sherman et al., 2001), the glider has a small wing and the induced drag is ignored. The drag is about 4N with the values in the above when $\mathbf{v} = 0$ and it corresponds to the acceleration of 0.04 m/s^2 ($\approx$ 4N/109kg). The acceleration, 0.04 m/s^2, is the possible maximum value when the glider is stationary. The acceleration caused by the current would be much smaller than the maximum as the glider usually does not fly in the exact opposite to the current. Then, these tiny current effect would be completely blocked by the sensor noise and the external fluctuations.

After the bias error in (23) is corrected in the previous section, given that the attitude error is small compared to the bias and the current effect on the acceleration measurement, the remaining uncorrected error in (23) is

$$\mathbf{w} \approx -C_{\mathcal{B}'}^{\mathcal{R}}\Delta\ddot{\mathbf{r}} = \frac{D}{m}\mathbf{e}_D \qquad (34)$$

where m is the mass of the glider and $\mathbf{e}_D$ is the unit vector towards the current direction. Sea current near the surface is mainly caused by wind and the temperature differences. Hence, the vertical direction is negligible in the near surface depth compared to the magnitudes of the horizontal direction components (Park et al., 2013). Hence,

$$\mathbf{e}_D = \begin{cases} \dfrac{\Delta\mathbf{v}}{\|\Delta\mathbf{v}\|}, & \text{for } \|\Delta\mathbf{v}\| > 0 \\ \mathbf{0}, & \text{otherwise} \end{cases} \qquad (35)$$

Compare the scales of acceleration in Figures 6 and 9, the one from the current drag is about 10-times smaller than the one from the accelerometer measurements. Hence, the effect of the current cannot be sensed by the accelerometer as it is completely submerged inside the sensor noise. However, its effect on the path are accumulated in the several hours of diving.

Table 1. Final position error ([km]) for the bias only fixed (B) and the bias with the sea current fixed using seven different current data

Day	1	2	3	4	5	6	7	B
Err	2.73	2.73	2.73	2.73	2.73	2.72	2.72	4.85

The path comparison between the one obtained by integrating the bias fixed only acceleration and the one by integrating the bias and the sea current fixed acceleration is shown in Figure 8. The total distance is shortened about 30% but the direction is correctly pointing toward the final position provided by GPS. The paths calculated using different current data are compared in Table 1 in terms of the distance from the estimated at the final and the one from GPS. The error reduced about 43% compared to the one without the current drag compensation.

4. CONCLUSIONS & FUTURE WORKS

Algorithms to correct various errors in the accelerometer output of underwater glider are presented. The algorithms do not require to investigate the built-in navigation systems of the glider, which is normally provided by the manufacturer or already installed on the glider. The algorithm corrects the bias error using the navigation system output and corrects further using the a priori information about the average current data over the operation area. The calculation results using the experimental data collected by KIOST in East Sea, Korea, demonstrate the performance of the algorithms.

The uncertainty boundary of the final GPS update position could be obtained by providing the ranges of several physical parameters, e.g., drag coefficient, mass, sea current changes, etc. The proposed algorithms can be implemented in on-board computer without requiring too much computational power. Moreover, for the case without having the current information, it can be still used recursively by estimating the current based on the position error measured every diving. Finally, the proposed algorithm could be used the predict the path of floating objects and the prediction would be exploited in the glider path planning to avoid any collision.

Although the algorithm shows some robustness towards the uncertainties in sea current data, it is, however, ideal to have more accurate and up to date information. In future, some real-time current data, e.g. OSCAR (Ocean Surface Current Analysis - Real time) project (National Oceanic and Atmospheric Administration, 2013), would be available and this could improve the algorithm performance in reduction the navigation error.

ACKNOWLEDGEMENTS

REFERENCES

Alaks Native Technologies, L. (2011). ANT analysis of KORDI LG19 flight. Technical Memo.

Davis, R.E., Eriksen, C.C., and Jones, C.P. (2002). *The Technology and Applications of Autonomous Underwater Vehicles*, chapter 2, Chapter 3. Autonomous Buoyancy–driven underwater gliders. Taylor & Francis.

Eriksen, C.C., Osse, T.J., Light, R.D., Wen, T., Lehman, T.W., Sabin, P.L., Ballard, J.W., and Chiodi, A.M. (2001). Seaglider: a long-range autonomous underwater vehicle for oceanographic research. *Oceanic Engineering, IEEE Journal of*, 26(4), 424–436.

Exocetus (2013). Exocetus. URL http://exocetus.com.

Griffiths, G., Davis, R., Erikson, C., Frye, P., Marchand, T., Dickey, T., and Weller, R. (2001). Towards new platform technology for sustained observations. In *First International Conference on Ocean Observations for Climate (OCEANOBS99)*, 324–337.

Imlach, J. and Mahr, R. (2012). Modification of a military grade glider for coastal scientific applications. In *Oceans, 2012*, 1–6. IEEE. doi: 10.1109/oceans.2012.6405134.

Korea Hydrographic & Oceanographic Administration (2011). East sea surface currents prediction model.

Lefferts, E.J., Markley, F.L., and Shuster, M.D. (1982). Kalman filtering for spacecraft attitude estimation. *Journal of Guidance, Control, and Dynamics*, 5(5), 417–429.

National Oceanic and Atmospheric Administration (2013). OSCAR near realtime global ocean surface currents. URL http://www.oscar.noaa.gov.

Park, Y., Lee, S., Lee, Y., Jung, S.K., Jang, N., and Lee, H.W. (2012). Report of east sea crossing by underwater glider. *Journal Of the Korean Society of Oceanography*, 130–137.

Park, Y.G., Park, J.H., Lee, H.J., Min, H.S., and Kim, S.D. (2013). The effects of geothermal heating on the East/Japan Sea circulation. *J. Geophys. Res. Oceans*, 118(4), 1893–1905. doi:10.1002/jgrc.20161.

Schaub, H. and Junkins, J. (2009). *Analytical Mechanics of Space Systems (AIAA Education Series)*. AIAA, 2 edition.

Sherman, J., Davis, R., Owens, W.B., and Valdes, J. (2001). The autonomous underwater glider "Spray". *Oceanic Engineering, IEEE Journal of*, 26(4), 437–446. doi:10.1109/48.972076.

Shuster, M.D. and Oh, S.D. (1981). Attitude determination from vector observations. *Journal of Guidance, Control, and Dynamics*, 4(1), 70–77.

Smith, R.N., Kelly, J., Chao, Y., Jones, B.H., and Sukhatme, G.S. (2010). Towards the improvement of autonomous glider navigational accuracy through the use of regional ocean models. In *Proc. ASME 2010 29th Int'l Conf. Ocean, Offshore and Arctic Engineering (OMAE'10)*. Shanghai, China.

Testor, P., Meyeres, G., and *et. al.* (2009). Gliders as a component of future observing systems. In *Proceedings of the OceanObs'09: Sustained Ocean Observations and Information for Society Conference (Vol. 2)*.

Ulanov, A.V. (2006). Underwater glider navigation in a nonhomogenous current. *Aerospace and Electronic Systems Magazine, IEEE*, 21(11), 27–28. doi: 10.1109/MAES.2006.284355.